# Toroidal plasmas

## Overview

- **Introduction:** Context is Alfvén wave dynamics, statement of equilibrium problem, cylindrical equilibrium, rotational transform, importance for stability;

- **Toroidal equilibrium:** Grad–Shafranov equation, scaling, Soloviev equilibrium, mapping to straight field line coordinates for stability;

- **Analysis of waves and instabilities:** toroidal wave equation, continuous spectra, toroidal Alfvén eigenmodes, field line resonances and ballooning modes;

- **Numerics of waves and instabilities:** numerical investigation of toroidal stability (ideal and resistive), edge-localized modes, MHD spectroscopy of tokamaks.

## Context: plasma dynamics

| time scale | tokamak | corona |  |
| --- | --- | --- | --- |
| very fast | $10^{-9}\,\mathrm{s}$ | $10^{-6}\,\mathrm{s}$ | $\Rightarrow$ *Kinetic waves & instabilities* |
| fast | $10^{-6}\,\mathrm{s}$ | $10\,\mathrm{s}$ | $\Rightarrow$ *MHD waves & instabilities* |
| slow | $10^{-3}\,\mathrm{s}$ | $10^{4}\,\mathrm{s}$ | $\Rightarrow$ *MHD equilibrium* |
| very slow | $1\,\mathrm{s}$ | $10^{11}\,\mathrm{s}$ | $\Rightarrow$ *Transport* |

$\Rightarrow$ **MHD range is the most robust part**

- **MHD equilibrium & stability:** absolute requirements for fusion in tokamaks.

- **MHD spectroscopy:** diagnostics of laboratory as well as astrophysical plasmas.

## Alfvén wave dynamics

- **Alfvén waves are point perturbations propagating along the magnetic field lines** (Friedrich's diagram).

  $\Rightarrow$ *Alfvén waves 'sample' the whole magnetic configuration* (global problem!).

- **The Alfvén frequency vanishes for $\mathbf{B} \cdot \nabla \sim k_{\parallel} = 0$.**

  $\Rightarrow$ *Stability hinges on the smallness of the $\mathbf{B} \cdot \nabla$ operator,* so that the equilibrium should be known extremely accurately to produce the required balancing of large terms in numerical stability codes.

## Statement of the equilibrium problem

- **To determine the magnetic confinement topology** (field lines, magnetic surfaces, curvatures, etc.) **of the 'most boring' case of plasma dynamics:**

  $\Rightarrow$ *Static equilibrium ($\mathbf{v}_0 = 0$) $\equiv$ absence of dynamics!*

## Nonlinear MHD equations

- Conservation of **Mass:**

$$\frac{\partial \rho}{\partial t} = -\nabla \cdot (\rho \mathbf{v}) , \tag{1}$$

- Conservation of **Momentum:**

$$\rho \left( \frac{\partial}{\partial t} + \mathbf{v} \cdot \nabla \right) \mathbf{v} = -\nabla p + (\nabla \times \mathbf{B}) \times \mathbf{B} , \tag{2}$$

- Conservation of **Entropy:**

$$\left( \frac{\partial}{\partial t} + \mathbf{v} \cdot \nabla \right) p = -\gamma p \nabla \cdot \mathbf{v} , \tag{3}$$

- Conservation of **Magnetic Flux:**

$$\frac{\partial \mathbf{B}}{\partial t} = \nabla \times (\mathbf{v} \times \mathbf{B}) , \qquad \nabla \cdot \mathbf{B} = 0 . \tag{4}$$

$$\Rightarrow \quad \rho(\mathbf{r}, t) , \ \mathbf{v}(\mathbf{r}, t) , \ p(\mathbf{r}, t) , \ \mathbf{B}(\mathbf{r}, t) .$$

## Static equilibrium equations

- MHD equations with $\partial/\partial t = 0$ an $\mathbf{v}_0 = 0$:

$$\mathbf{j} \times \mathbf{B} = \nabla p \quad \textit{(pressure balance)}, \tag{5}$$

$$\mathbf{j} = \nabla \times \mathbf{B} \quad \textit{(Ampère's law)}, \tag{6}$$

$$\nabla \cdot \mathbf{B} = 0 \quad \textit{(THE law of magnetic fields)}. \tag{7}$$

- BC:

$$\mathbf{n} \cdot \mathbf{B} = 0 \quad \textit{(at prescribed boundary)}. \tag{8}$$

$\Rightarrow$ **Nonlinear problem with an enormous amount of freedom:**

- distribution of pressure and magnetic field,

- shape of the boundary.

$\Rightarrow$ **Different alternatives for fusion experiments:**

- pinches (1960) $\Rightarrow$ tokamaks/stellarators (1990) $\Rightarrow$ future devices (2020?).

# Cylinder symmetry

- **Rotation/translation symmetry:** $\partial/\partial\theta = 0$, $\partial/\partial z = 0$ $\Rightarrow$ $B_r = 0$, $j_r = 0$.

- Profiles: $\rho(r)$ arbitrary, $p(r)$, $B_\theta(r)$, $B_z(r)$ *restricted by equilibrium:*

$$\left.\begin{aligned}\frac{dp}{dr} &= j_\theta B_z - j_z B_\theta \\[2mm] j_\theta &= -\frac{dB_z}{dr}B_z, \quad j_z = \frac{1}{r}\frac{d}{dr}(rB_\theta)\end{aligned}\right\} \Rightarrow \frac{d}{dr}(p + \tfrac{1}{2}B^2) = -\frac{B_\theta^2}{r}, \qquad (9)$$

so that two of these profiles are arbitrary.

- For tokamaks, total pressure dominated by contribution of *magnetic pressure:*

$$\beta \equiv \frac{2p_0}{B_0^2} \ll 1 \quad \Rightarrow \quad P \equiv p + \tfrac{1}{2}B^2 \approx \tfrac{1}{2}B^2. \qquad (10)$$

Numbers:

$$B = 3\,\mathrm{T} \quad \Rightarrow \quad P = 3.6 \times 10^6\,\mathrm{N/m^2} = 360\,\text{metric tons} = 36\,\mathrm{atm}\ \text{(on the coils)!}$$

$$\beta = 0.03 \quad \Rightarrow \quad p \approx 1\,\mathrm{atm}\ \text{(internally, to be increased in future reactor).}$$

## Cylindrical equilibria

- Typical equilibrium profiles for:
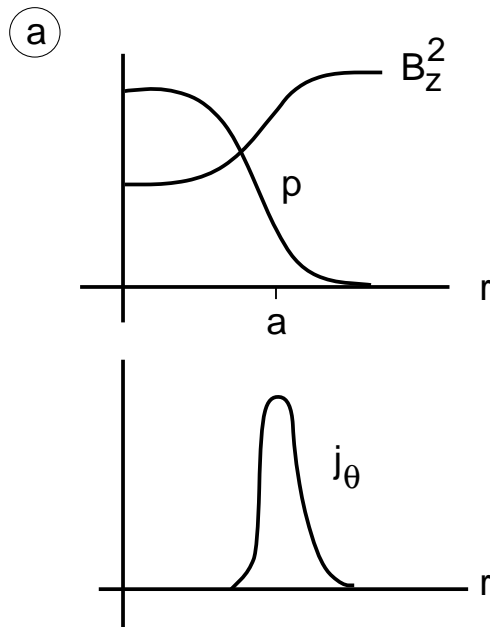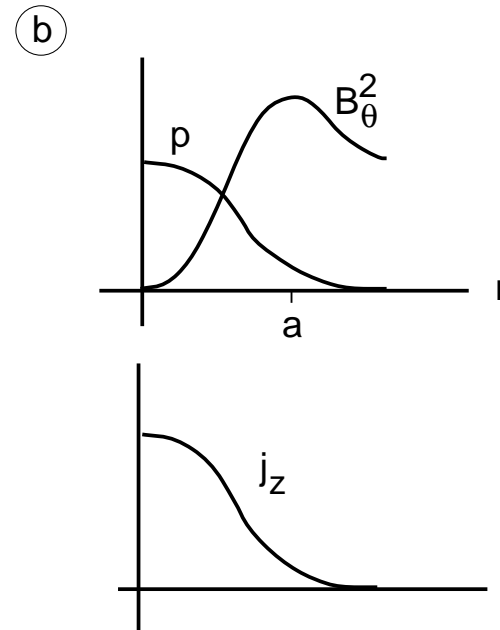


$$p + \tfrac{1}{2}B_z^2 = \text{const} \qquad\qquad p + \tfrac{1}{2}B_\theta^2 = \text{const} - \int (B_\theta^2/r)\, dr$$

- **'Straight tokamak'** (periodic cylinder model of torus): combined $\theta$–pinch (dominant $B_z \sim B_0$) and $z$-pinch (small $B_\theta \sim \epsilon B_0$), with much reduced pressure ($p \sim \epsilon^2$).

## Rotational transform (periodic cylinder)

- Definition:

$$q_{\text{cyl}} \equiv \frac{rB_z}{R_0 B_\theta} \quad \left( = \frac{2\pi r^2 B_z}{R_0 I_z} \right) . \tag{11}$$

- If **rational:**

$$q_{\text{cyl}} = \frac{N}{M} \quad \left( = \frac{\text{number of toroidal revolutions}}{\text{number of poloidal revolutions}} \right) . \tag{12}$$

ⓐ                                                                                    ⓑ

$2\pi R_0$

**B**

$q \cdot 2\pi R_0$

$0 \qquad\qquad 2\pi r$
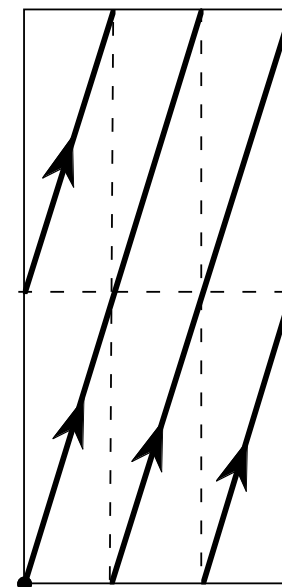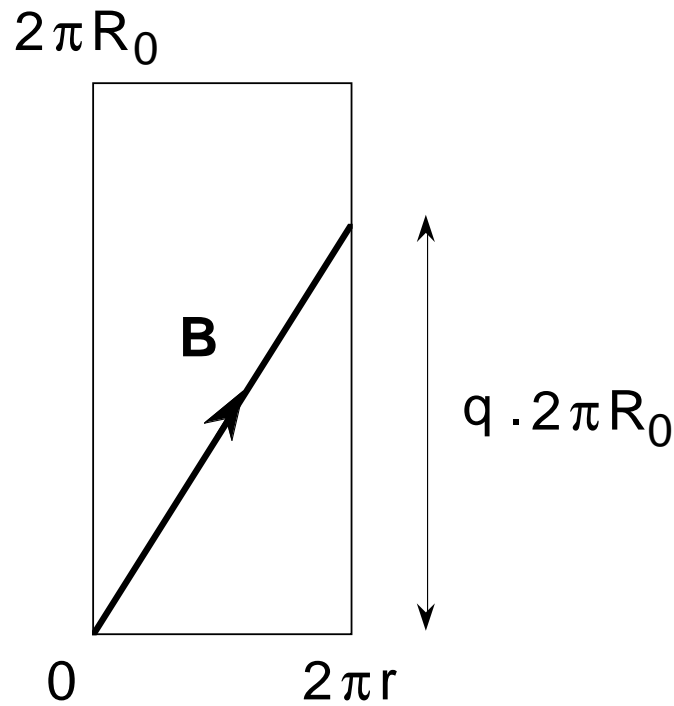
Cylindrical safety factor ($q < 1$)          Rational field line ($q = 3/2$)

## Rotational transform (cont'd)

- Perturbation on magnetic surface:

$$\sum_{m}\sum_{n}\xi_{mn}(r)\,\mathrm{e}^{\mathrm{i}(m\vartheta+n\varphi)}\,, \tag{13}$$

*with poloidal angle $\vartheta \equiv \theta$, toroidal angle $\varphi \equiv z/R_0$, toroidal mode number $n \equiv kR_0$.*

- **Parallel gradient operator:**

$$\mathbf{B}\cdot\nabla\xi \sim \mathbf{k}\cdot\mathbf{B}\,\xi \sim (m+nq)\,\xi\,. \tag{14}$$

$\Rightarrow$ **Rational field lines** with resonant perturbations crucial for instabilities:

$$q_{\mathrm{cyl}} = -\frac{m}{n} \quad \left(= -\frac{\text{poloidal mode number}}{\text{toroidal mode number}}\right)\,. \tag{15}$$

- Orders of magnitude for periodic cylinder representing toroidal tokamak:

$$\epsilon \equiv a/R_0 \ll 1\,, \quad B_\theta/B_0 \sim \epsilon\,, \quad B_z/B_0 \sim 1 \quad \Rightarrow q_{\mathrm{cyl}} \sim 1\,. \tag{16}$$

- **Pressure effects,** represented by $\beta \equiv 2p_0/B_0^2 \sim \epsilon^2 \ll 1$, are not properly described by cylindrical approximation $\Rightarrow$ **require genuine toroidal theory.**

## 'Straight tokamak': q determines stability
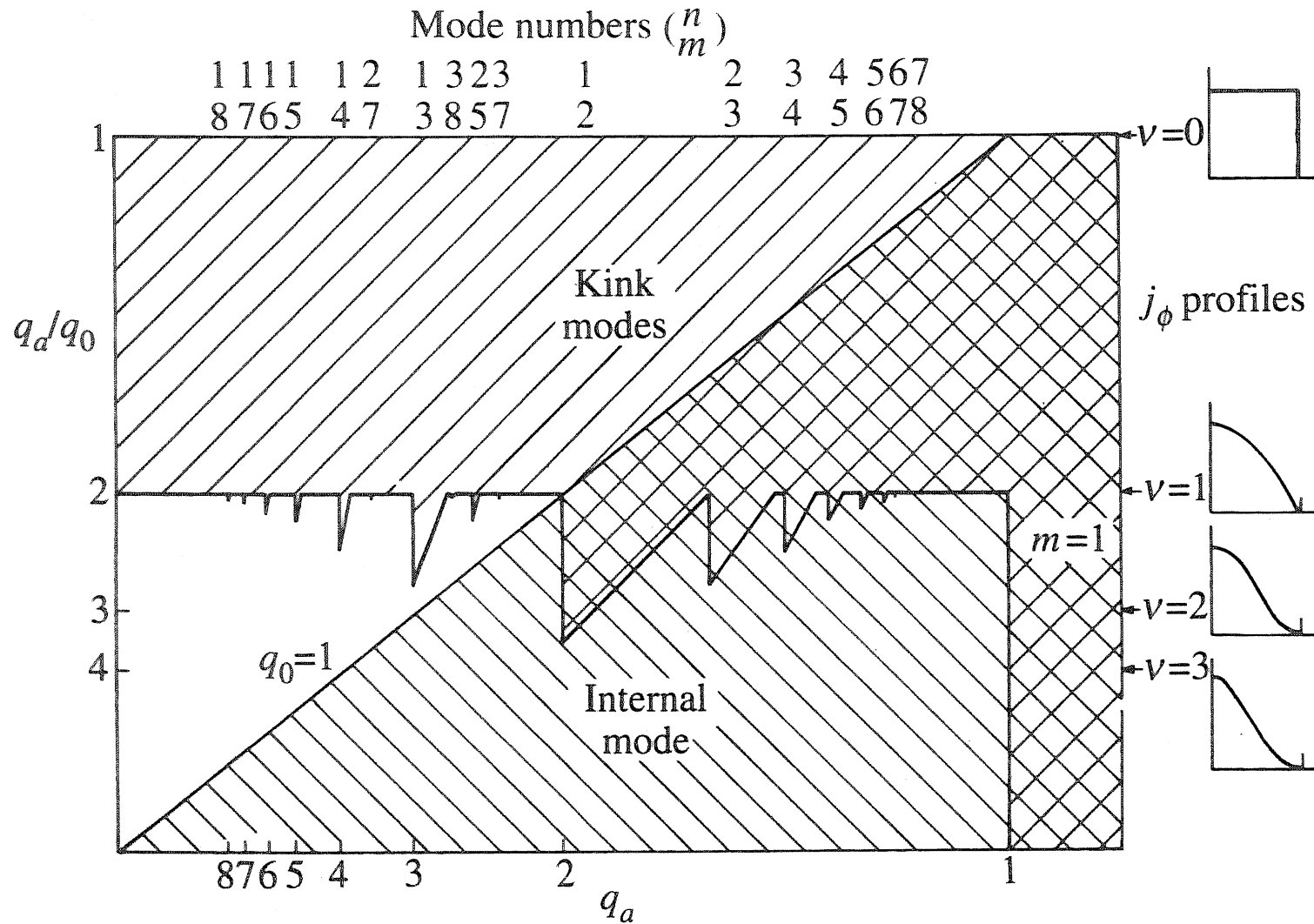


[Wesson, Nuclear Fusion **18**, 87 (1978)]

## Toroidal equilibrium: poloidal field

**Consequences of axisymmetry** ($\partial/\partial\varphi = 0$, using modified cyl. coordinates $R$, $Z$, $\varphi$):

- THE law of magnetic fields (7) integrated by means of the vector potential:

$$\nabla \cdot \mathbf{B} = 0 \quad \Rightarrow \quad \mathbf{B} = \nabla \times \mathbf{A}\,. \tag{17}$$

Toroidal component related to **poloidal magnetic flux** (renormalized with factor $2\pi$) through area bounded by the *magnetic axis* (where $\Psi = 0$) and circle of radius $R$:

$$\Psi \equiv \frac{1}{2\pi} \iint \mathbf{B} \cdot \mathbf{n}\, dS \overset{\text{(Stokes)}}{=} \frac{1}{2\pi} \oint \mathbf{A} \cdot d\boldsymbol{l} = -\frac{R}{2\pi} \int_0^{2\pi} A_\varphi\, d\varphi = -R A_\varphi \tag{18}$$

$$(17) \quad \Rightarrow \quad B_R = -\frac{1}{R}\frac{\partial\Psi}{\partial Z}, \quad B_Z = \frac{1}{R}\frac{\partial\Psi}{\partial R} \quad \Rightarrow \quad \mathbf{B}_p = \frac{1}{R}\mathbf{e}_\varphi \times \nabla\Psi\,. \tag{19}$$

$\Psi$ labels the **magnetic surfaces** spanned by $\mathbf{B}$ and $\mathbf{j}$ with $\nabla p$ orthogonal to them.

- If Poisson bracket of a function $F$ with $\Psi$ vanishes, that function is a **flux function:**

$$\{F, \Psi\} \equiv \mathbf{e}_\varphi \cdot (\nabla F \times \nabla\Psi) = \frac{\partial F}{\partial R}\frac{\partial\Psi}{\partial Z} - \frac{\partial F}{\partial Z}\frac{\partial\Psi}{\partial R} = 0 \quad \Rightarrow \quad F = F(\Psi)\,. \tag{20}$$

## Toroidal equilibrium: current

- From Ampere's law (6), **poloidal current** derives from *stream function $I(R, Z)$ related to toroidal magnetic field:*

$$\mathbf{j} = \nabla \times \mathbf{B} \quad \Rightarrow \quad \nabla \cdot \mathbf{j} = 0 \tag{21}$$

$$\Rightarrow \quad j_R = \frac{\partial B_\varphi}{\partial Z} = \frac{1}{R}\frac{\partial I}{\partial Z}, \quad j_Z = -\frac{1}{R}\frac{\partial(RB_\varphi)}{\partial R} = -\frac{1}{R}\frac{\partial I}{\partial R} \tag{22}$$

$$\Rightarrow \quad \mathbf{j}_p = -\frac{1}{R}\mathbf{e}_\varphi \times \nabla I, \qquad I \equiv RB_\varphi. \tag{23}$$

- From Ampere's law (6), **toroidal current density** related to *poloidal flux:*

$$Rj_\varphi = R\left(\frac{\partial B_Z}{\partial R} - \frac{\partial B_R}{\partial Z}\right) = R\frac{\partial}{\partial R}\left(\frac{1}{R}\frac{\partial\Psi}{\partial R}\right) + \frac{\partial^2\Psi}{\partial Z^2} \equiv \Delta^*\Psi \tag{24}$$

$$\text{(quasi-Laplacian)}.$$

- From toroidal force balance equation (5), $I$ **is a flux function**:

$$\frac{\partial p}{\partial \varphi} = j_R B_Z - j_Z B_R = -\frac{1}{R^2}\{I, \Psi\} = 0 \quad \Rightarrow \quad I \equiv I(\Psi), \tag{25}$$

## Toroidal equilibrium: force balance

- From poloidal force balance equation (5), $p$ **is a flux function**:

$$\frac{\partial p}{\partial R} = j_Z B_\varphi - j_\varphi B_Z = \left( -\frac{II'}{R^2} - \frac{j_\varphi}{R} \right) \frac{\partial \Psi}{\partial R}$$

$$\frac{\partial p}{\partial Z} = j_\varphi B_R - j_R B_\varphi = \left( -\frac{II'}{R^2} - \frac{j_\varphi}{R} \right) \frac{\partial \Psi}{\partial Z} \quad \Rightarrow \quad \begin{cases} p = p(\Psi), \\[2mm] -\dfrac{II'}{R^2} - \dfrac{j_\varphi}{R} = p'. \end{cases} \quad (26)$$

- From (24) and (26)(b), **equilibrium described by Grad–Shafranov equation:**

$$[\,\Delta^* \Psi \equiv\,] \quad R\frac{\partial}{\partial R}\left( \frac{1}{R}\frac{\partial \Psi}{\partial R} \right) + \frac{\partial^2 \Psi}{\partial Z^2} = -II' - R^2 p' \quad [\,= R j_\varphi\,], \qquad (27)$$

which is an elliptic nonlinear PDE that has to satisfy BC

$$\Psi = \text{const} \quad \text{(on outer plasma cross-section: the wall)}. \qquad (28)$$

- Note that $p(\Psi)$ *and* $I(\Psi)$ *are completely arbitrary functions,* not determined by anything in the equilibrium: they should be provided by experimental diagnostics (and controlled by machine operators!).

# Uncertainty
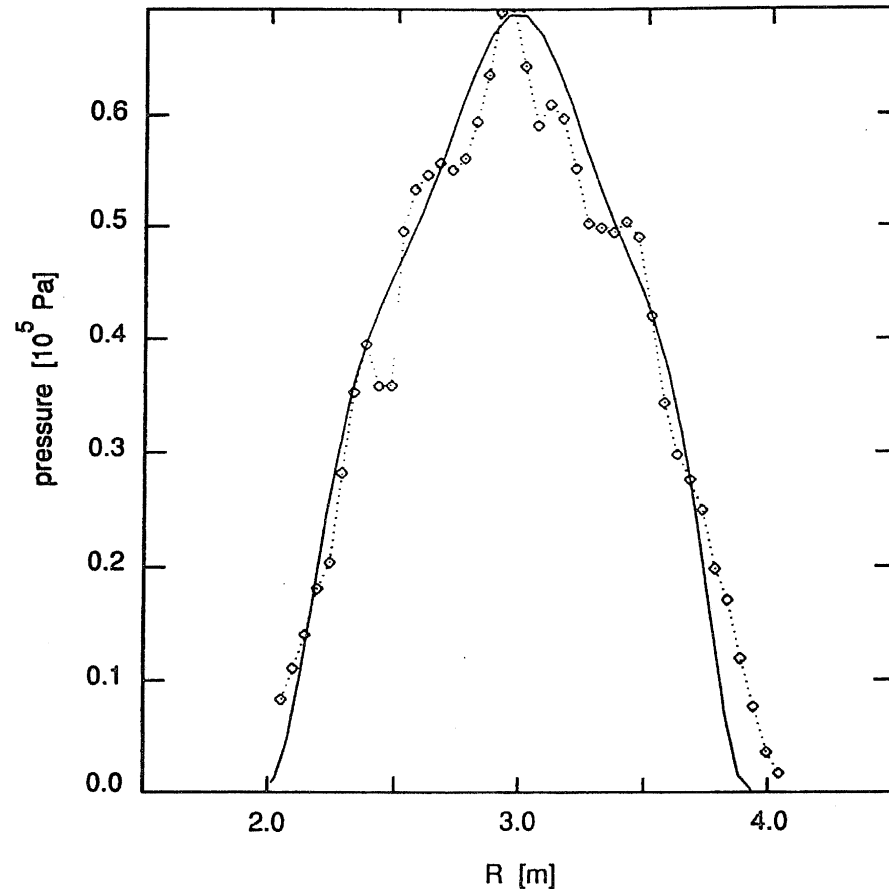


*Smoothing experimental data to obtain equilibrium profiles for stability studies:*

- inaccurate experimental data

  or

- neglecting essential 3D deviations (magnetic islands) from axisymm.?

Electron pressure profile obtained by LIDAR diagnostic at JET (dashed with diamonds) and reconstructed pressure profile by means of an equilibrium solver (drawn).

[Huysmans et al., Phys. Fluids **B5**, 1545 (1993)]

## Scaling the geometry
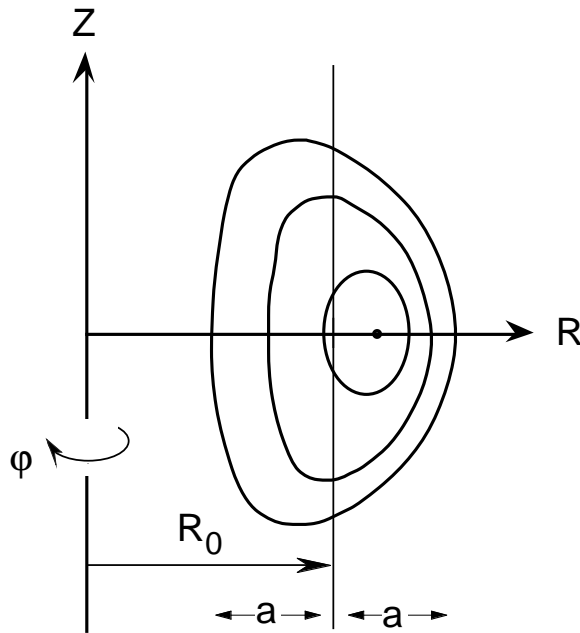


Cross-sectional shape                    poloidal $x$-$y$ plane.
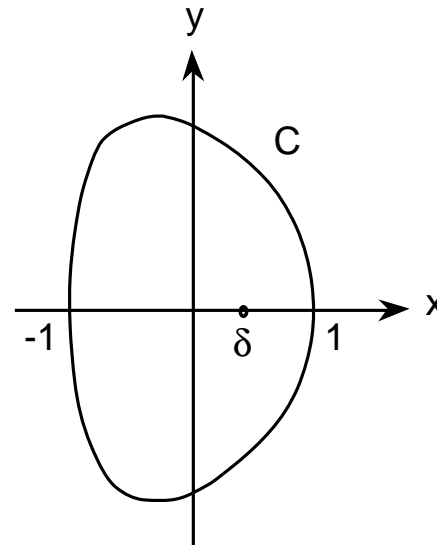
- Map to *Cartesian coordinates:* $\quad x \equiv (R - R_0)/a \,, \quad y \equiv Z/a \,.$ $\qquad$ (29)

- Exploit *inverse aspect ratio:* $\qquad \epsilon \equiv a/R_0 \quad (\ll 1 \text{ in asymptotic expansions}).$ (30)

## Scaling the physical variables

- Define *unit flux label* by dividing $\Psi$ through total poloidal flux through the plasma:

$$\tilde{\psi} \equiv \Psi/\Psi_1 \quad \Rightarrow \quad 0 \le \tilde{\psi} \le 1 \,, \tag{31}$$

and *dimensionless inverse flux* (related to safety factor on edge):

$$\alpha \equiv a^2 B_0/\Psi_1 \; (\sim q_1) \,. \tag{32}$$

- Split profiles in *(arbitrary) unit profiles and amplitudes* $A$ and $B$:

$$\frac{\alpha}{B_0}\left[\, II' + \frac{a^2}{\epsilon^2}\, p'\,\right] \equiv -A\Gamma(\tilde{\psi})\,, \qquad \Gamma(0) = 1\,, \quad \Gamma(1) = 0\,, \tag{33}$$

$$\frac{\alpha a^2}{\epsilon B_0}\, p' \equiv -\tfrac{1}{2}AB\Pi(\tilde{\psi})\,, \qquad \Pi(0) = 1\,, \quad \Pi(1) = 0\,.$$

- The **Grad–Shafranov equation** then becomes:

$$\tilde{\psi}_{xx} + \tilde{\psi}_{yy} - \epsilon(1+\epsilon x)^{-1}\,\tilde{\psi}_x = A[\,\Gamma(\tilde{\psi}) + Bx(1+\tfrac{1}{2}\epsilon x)\Pi(\tilde{\psi})\,]\,, \tag{34}$$

with BCs:
$$\tilde{\psi} = 1 \qquad\qquad \text{at plasma boundary } C \; (r = f(\theta))\,, \tag{35}$$

$$\tilde{\psi} = \tilde{\psi}_x = \tilde{\psi}_y = 0 \quad \text{at magnetic axis} \quad (x = \delta,\; y = 0)\,. \tag{36}$$

$\Rightarrow$ Now, for given $\delta$, $A$ and $B$ are *eigenvalues* to be determined together with $\tilde{\psi}$.

## The two main parameter of tokamaks

- **The 'safety factor' $q$ determines the magnetic structure:**

$$q(\Psi) \equiv \frac{1}{2\pi} \oint \frac{d\varphi}{d\theta}\bigg|_{\text{field line}} d\theta \,, \tag{37}$$

  where $\theta$ is some polar angle in the poloidal plane (more on that later).

- **The plasma $\beta$ determines the power output of a future fusion reactor:**

$$\beta \equiv \frac{2\mu_0 \langle p \rangle}{\langle B^2 \rangle} \quad \Rightarrow \quad \beta_p \equiv \frac{2\mu_0 \langle p \rangle}{\langle B_p^2 \rangle} \sim \frac{\beta}{I_\varphi^2} \sim \beta q_1^2 \,, \tag{38}$$

  with averages taken over the plasma volume.

- They need to be optimized together (which has been quite successful in tokamaks): **Equilibrium** *determines value of $\beta_p$,* **Stability** *determines operating ranges for $q$* (limited by current driven instabilities) *and $\beta$* (limited by pressure driven instabilities).

- Ordering in inverse aspect ratio:

$$\epsilon \beta_p \sim \frac{1}{\epsilon} \beta \, q_1^2 \quad \Rightarrow \quad \begin{cases} \text{\textit{low-}$\beta$ \textit{tokamak}} : \beta \sim \epsilon^2 \,,\ \epsilon \beta_p \sim \epsilon \,, \\ \text{\textit{'high-}$\beta$' \textit{tokamak}} : \beta \sim \epsilon \,,\ \epsilon \beta_p \sim 1 \,. \end{cases} \tag{39}$$

# Equilibrium solver: counting parameters

|  | **Input** | **Solver** | **Output** |
|---|---|---|---|

scaled pol. flux $\quad \tilde{\psi}_1 (\equiv 1)$

shift magn. axis $\quad \delta$

cross section $\quad \boxed{C, f(\theta)}$

inv. aspect ratio $\quad \boxed{\epsilon}$ $\qquad \Longrightarrow$

'toroidal current' $\quad \boxed{\Gamma(\tilde{\psi})}$

pressure gradient $\quad \boxed{\Pi(\tilde{\psi})}$

inverse pol. flux $\quad \boxed{\alpha}$

Solver box:
$A \quad \rightarrow \quad \boxed{\tilde{q}_1}$
$\tilde{\psi}(x, y)$
$B \quad \rightarrow \quad \boxed{\epsilon\beta_p}$

$\Longrightarrow$

Output box:
$q_1 \qquad q$ on edge
$\beta/\epsilon \qquad$ scaled $\beta$
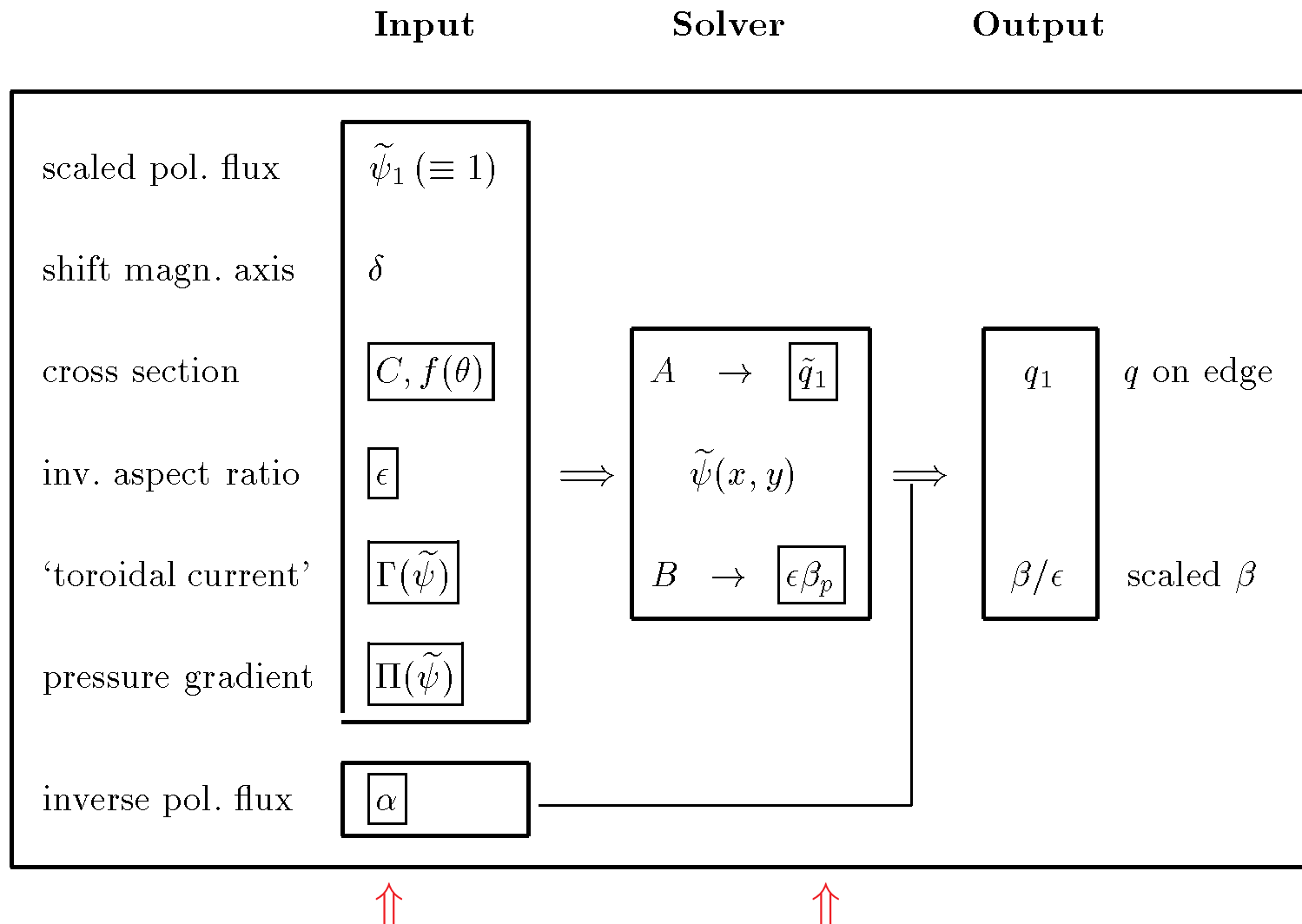
7 independent parameters and profiles in the small boxes:
since $\tilde{\psi}_1 \equiv 1$ and $\delta$ are prescribed, eigenvalues $A$ and $B$ determine $\tilde{q}_1 \equiv q_1/\alpha$ and $\epsilon\beta_p$.

# Example: Soloviev equilibrium

- **Linearize** Grad–Shafranov equation by choosing constant $\Gamma(\tilde{\psi}) \equiv \Pi(\tilde{\psi}) \equiv 1$:

$$\tilde{\psi}_{xx} + \tilde{\psi}_{yy} - \epsilon(1 + \epsilon x)^{-1}\,\tilde{\psi}_x = A\left[1 + Bx(1 + \tfrac{1}{2}\epsilon x)\right]. \tag{40}$$

- This yields a three parameter family of solutions:

$$\tilde{\psi} = \left[\, x - \tfrac{1}{2}\epsilon(1 - x^2)\,\right]^2 + \left[\,(1 + \lambda - \tfrac{1}{4}\epsilon^2)(1 + \epsilon x)^2 - \lambda\,\right]\left(\frac{a}{b}\,y\right)^2, \tag{41}$$

  where $\epsilon$ **is the inverse aspect ration,** $b/a$ **the elongation, and** $\lambda$ **the triangularity** of the flux surfaces. This also fixes the constants $A$ and $B$:

$$A = 2(a^2/b^2)\left[\,1 + b^2/a^2 - \tfrac{1}{4}\epsilon^2\,\right], \qquad B = 2\epsilon\left[\,1 + \frac{\lambda}{1 + b^2/a^2 - \tfrac{1}{4}\epsilon^2}\,\right]. \tag{42}$$

  Note that we did not impose the shape of the boundary or the position of the magnetic axis, but just let these follow from the polynomial form chosen by Soloviev.

- Now, we can compute everything that is of physical interest for a toroidal equilibrium.

# Soloviev equilibrium: special points

- **Elliptic and hyperbolic points** of the flux surfaces:

$$\Delta \equiv \tilde{\psi}_{xx}\tilde{\psi}_{yy} - 4\tilde{\psi}_{xy}^2 \quad \Rightarrow \quad \begin{cases} \Delta > 0 : & \text{elliptic}, \\ \Delta < 0 : & \text{hyperbolic}. \end{cases} \tag{43}$$

- The **magnetic axis** should be elliptic for closed flux surfaces:

$$x_m \equiv \delta = \frac{1}{\epsilon}\left(\sqrt{1+\epsilon^2} - 1\right), \qquad y_m = 0. \tag{44}$$

- A **second magnetic axis** (elliptic for $\lambda > 0$, hyperbolic for $\lambda < 0$) occurs at the origin of the original $R, Z$ coordinate system:

$$x_0 = -\frac{1}{\epsilon}, \qquad y_0 = 0. \tag{45}$$

Hyperbolic points are found at the intersections of the **separatrices:**

$$x_s = -\frac{1}{\epsilon} + \frac{1}{\epsilon}\sqrt{\frac{\lambda}{1+\lambda-\frac{1}{4}\epsilon^2}}, \qquad y_s = \pm\frac{b}{a}\sqrt{\frac{(1+\epsilon^2)(1-\frac{1}{4}\epsilon^2)+\epsilon^2\lambda}{2\epsilon^2(1+\lambda-\frac{1}{4}\epsilon^2)^2}}. \tag{46}$$

The latter two lie outside the physical region, but they determine the geometry of the flux surfaces there. The physical ranges of $\lambda$ may be found from these expressions.

## FORTRAN program Solo: plotting flux contours

- **Download Solo.tar.bz2 from**

  ftp://ftp.astro.iag.usp.br/pub/goedbloed/
  or
  www.rijnh.nl/users/goedbloed

- The following files are stored in programSolo/src:

  Solo.f – Fortran source of program Solo

  ppplib.f – Fortran source of plotting library ppplib (with contour plotter cplot)
  Makefile – Makefile to compile Solo and ppplib

- A typical sequence of commands is as follows:

  *cd programSolo/src* – Change to subdirectory src.
  *make Solo* – Compile ppplib & Solo and create executable "Solo".
  *make clean* – Clean out directory src again.
  *cd ..* – Change to main directory programSolo where you find the executable Solo.
  *./Solo* – Executing Solo from here results in a plot file Solo.ps.

- On the following page you find output of Solo for some values of the parameters. Change those and figure out how you can 'stuff' plasma up to the separatrices. (Recall that $\tilde{\psi} = 1$ was supposed to be the plasma boundary.)

# Soloviev equilibrium:  contours of $\sqrt{\tilde{\psi}}$

eps=  0.40,  boa=  1.00,  lam=  -4.50

eps=  0.40,  boa=  1.00,  lam=  -1.50

eps=  0.40,  boa=  1.00,  lam=   1.00

eps=  0.40,  boa=  1.00,  lam=   2.00
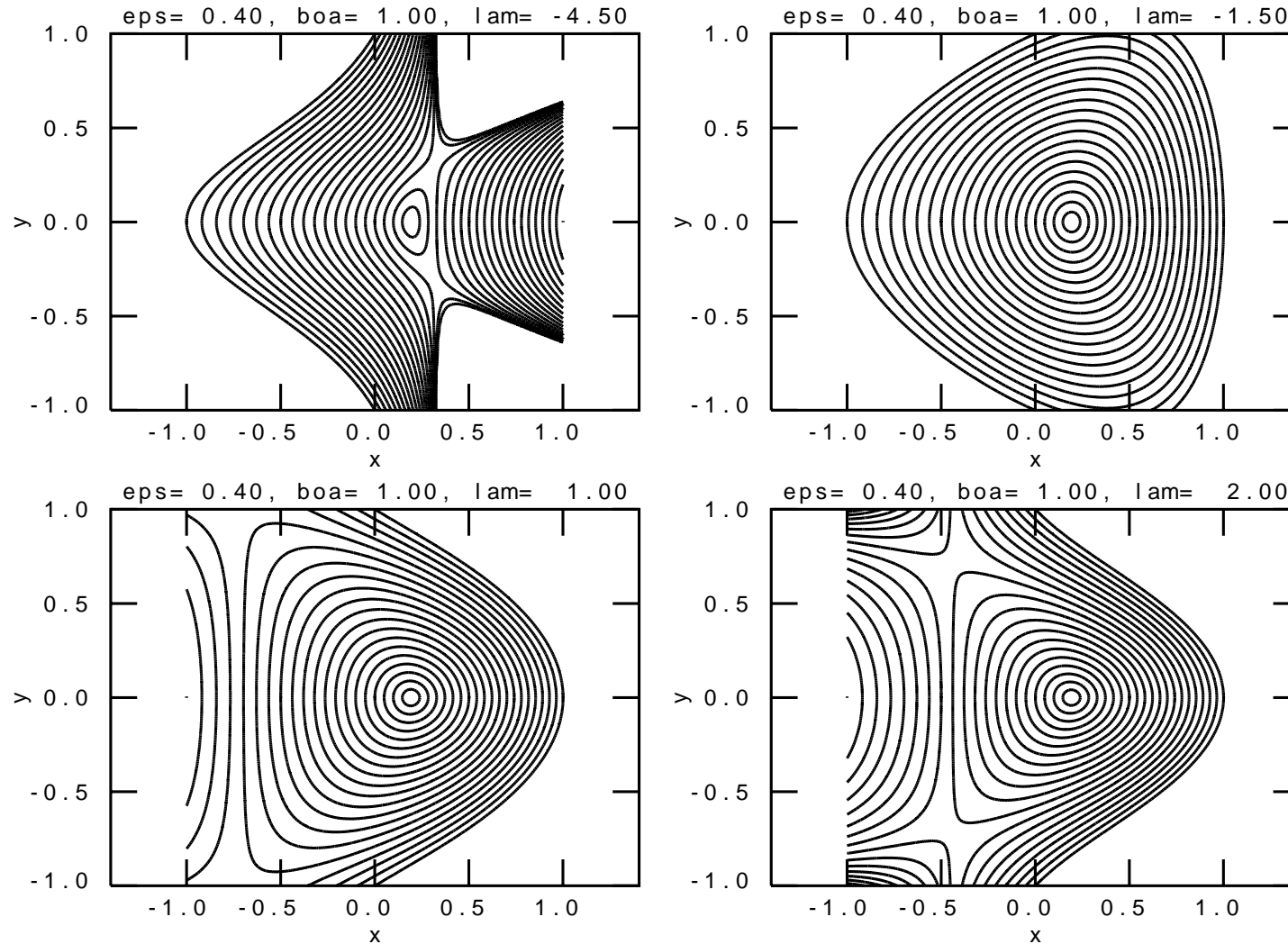
P r o g r a m   S o l o

## Straight field line coordinates

*Here, we exploit the unscaled, but dimensionless, flux $\psi \equiv \Psi/(a^2 B_0)$!*

- **Spectral analysis** requires coordinate inversion:

$$\begin{aligned}\psi &= \psi(x_i, y_j) \\ \theta &= \theta(x_i, y_j)\end{aligned} \quad \Rightarrow \quad \begin{aligned}x &= x(\psi_i, \theta_j) \\ y &= y(\psi_i, \theta_j)\end{aligned}.$$

- **Representation of parallel gradient operator** $\mathbf{B} \cdot \nabla \sim m + nq$ requires 'straight field lines':

$$\theta \quad \rightarrow \quad \vartheta \equiv \frac{1}{q} \int_0^\theta \nu(\psi, \theta)\, d\theta, \qquad (47)$$

such that the variable 'direction' of a field line,

$$\nu(\psi, \theta) \equiv \left. \frac{d\varphi}{d\theta} \right|_{\text{field line}},$$

becomes the constant **rotational transform**

$$q(\psi) \equiv \left. \frac{d\varphi}{d\vartheta} \right|_{\text{field line}}. \qquad (48)$$
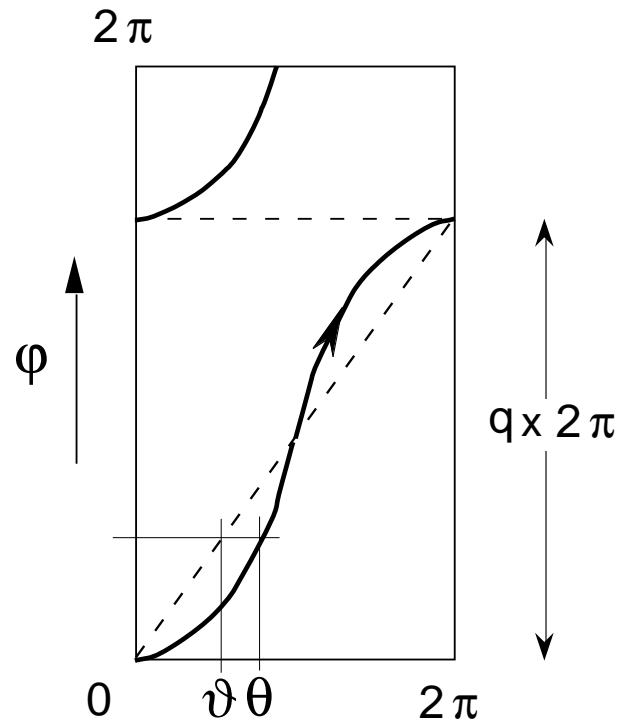


Construction of angle $\vartheta$ from $\theta$

- **All equilibrium quantities are transformed to** $(\psi, \vartheta, \varphi)$ **coordinates,** e.g. field line and magnetic surface curvatures, toroidal current, etc. ($\sim$ 2nd derivatives w.r.t. $\psi$).

  $\Rightarrow$ **Equilibrium needs to be surprisingly accurate for reliable stability analysis.**

## Non-orthogonal coordinates

- To exploit the non-orthogonal coordinates $(\psi, \vartheta, \varphi)$, one needs to connect Cartesian coordinates $(X, Y, Z)$ centered at toroidal axis to $(x, y)$ coordinates of poloidal plane:

$$
\begin{cases}
X = R \sin \varphi, & R = R_0 + x(\psi, \vartheta), \\
Y = R \cos \varphi, \\
Z = y(\psi, \vartheta),
\end{cases}
\tag{1}
$$

where the poloidal dependence is obtained from inversion of the equilibrium solution:

$$
\text{equilibrium} \;\Rightarrow\;
\begin{cases}
\psi = \psi(x, y) \\
\vartheta = \vartheta(x, y)
\end{cases}, \qquad
\text{inversion} \;\Rightarrow\;
\begin{cases}
x = x(\psi, \vartheta) \\
y = y(\psi, \vartheta)
\end{cases}.
\tag{2}
$$

- This yields the **metric of the non-orhogonal coordinates** $(\psi, \vartheta, \varphi)$:

$$
g_{ij} = \begin{pmatrix} g_{11} & g_{12} & 0 \\ g_{12} & g_{22} & 0 \\ 0 & 0 & g_{33} \end{pmatrix},
\qquad
\begin{aligned}
g_{11} &= (x_\psi)^2 + (y_\psi)^2, \\
g_{12} &= x_\psi \, x_\vartheta + y_\psi \, y_\vartheta, \\
g_{22} &= (x_\vartheta)^2 + (y_\vartheta)^2, \\
g_{33} &= R^2 = (R_0 + x)^2,
\end{aligned}
\tag{3}
$$

where the Jacobian,

$$
J = (\nabla \psi \times \nabla \vartheta \cdot \nabla \varphi)^{-1} = R \sqrt{g_{11} g_{22} - (g_{12})^2} = R \, (x_\psi \, y_\vartheta - x_\vartheta \, y_\psi),
\tag{4}
$$

has a simply relation to $q$ **for 'straight' field line coordinates:** $J = q(\psi) R^2 / I(\psi)$.

## Toroidal wave equation

- Linearise the MHD equations:

$$f(\mathbf{r}, t) \approx f_0(\psi, \vartheta) + f_1(\psi, \vartheta)e^{i(n\varphi - \omega t)}, \tag{1}$$

where $n$ is the toroidal mode number.

- Exploit **projection on magnetic surfaces and field lines,** involving field line triad

$$\mathbf{n} \equiv \nabla\psi / |\nabla\psi|, \quad \boldsymbol{\pi} \equiv \mathbf{b} \times \mathbf{n}, \quad \mathbf{b} \equiv \mathbf{B}/B. \tag{2}$$

$\Rightarrow$ Gradient operator:

$$\begin{aligned}
D &\equiv (RB_p)^{-1}\mathbf{n} \cdot \nabla &&\Rightarrow \partial_\psi - (g_{12}/g_{22})\,\partial_\vartheta, \\
G &\equiv -i\mathbf{B} \times \nabla\psi \cdot \nabla &&\Rightarrow -iI J^{-1}\partial_\vartheta - nB_p^2, \\
F &\equiv -i\mathbf{B} \cdot \nabla &&\Rightarrow J^{-1}(-i\partial_\vartheta + nq).
\end{aligned} \tag{3}$$

(Watch out: effects of $\nabla$ on basis vectors not represented here!)

$\Rightarrow$ Displacement vector:

$$X \equiv RB_p\,\boldsymbol{\xi} \cdot \mathbf{n}, \quad Y \equiv \frac{i}{RB_p}\boldsymbol{\xi} \cdot \boldsymbol{\pi}, \quad Z \equiv \frac{i}{B}\boldsymbol{\xi} \cdot \mathbf{b}. \tag{4}$$

- This yields the **toroidal wave equation:**

[Goedbloed, Phys. Fluids **18**, 1258 (1975); Trans. Fusion Science & Technology **45**, 95 (2004)]

$$
\begin{pmatrix}
\mathcal{A}_{11} & \mathcal{A}_{12} & \mathcal{A}_{13} \\
\mathcal{A}_{21} & \mathcal{A}_{22} & \mathcal{A}_{23} \\
\mathcal{A}_{31} & \mathcal{A}_{32} & \mathcal{A}_{33}
\end{pmatrix}
\begin{pmatrix}
X \\ Y \\ Z
\end{pmatrix}
= -\rho \omega^2
\begin{pmatrix}
\mathcal{B}_{11} X \\
\mathcal{B}_{22} Y \\
\mathcal{B}_{33} Z
\end{pmatrix},
\tag{5}
$$

with

$$
\mathcal{A}_{11} \equiv D(\gamma p + B^2)D^\dagger - F\frac{1}{R^2 B_p^2}F - E(\kappa_p, \kappa_t)\,, \qquad \mathcal{A}_{31} \equiv -F\gamma p D^\dagger\,,
$$

$$
\mathcal{A}_{12} \equiv DG\frac{\gamma p + B^2}{B} - 2\left(\frac{B_\varphi \kappa_t}{B_p}\frac{\mathrm{i}}{J}\partial_\vartheta + \frac{B_p \kappa_p}{R}n\right)B\,, \qquad \mathcal{A}_{32} \equiv -F\gamma p G\frac{1}{B}\,,
$$

$$
\mathcal{A}_{13} \equiv D\gamma p F\,, \qquad\qquad\qquad\qquad\qquad\qquad\qquad \mathcal{A}_{33} \equiv -F\gamma p F\,,
$$

$$
\mathcal{A}_{21} \equiv -\frac{\gamma p + B^2}{B}GD^\dagger - 2B\left(\frac{\mathrm{i}}{J}\partial_\vartheta\frac{B_\varphi \kappa_t}{B_p} + n\frac{B_p \kappa_p}{R}\right)\,, \quad \mathcal{B}_{11} \equiv \frac{1}{R^2 B_p^2}\,,
$$

$$
\mathcal{A}_{22} \equiv -\frac{1}{B}G\gamma p G\frac{1}{B} - BG\frac{1}{B^2}GB - BF\frac{R^2 B_p^2}{B^2}FB\,, \qquad \mathcal{B}_{22} \equiv R^2 B_p^2\,,
$$

$$
\mathcal{A}_{23} \equiv -\frac{1}{B}G\gamma p F\,, \qquad\qquad\qquad\qquad\qquad\qquad \mathcal{B}_{33} \equiv B^2\,.
$$

## Further directions

- **Continuous spectra** (local to magnetic surfaces):

    $\Rightarrow$ *obtained from the limit $D \to \infty$.*

- **Ballooning modes** (local to field lines):

    $\Rightarrow$ *more subtle limit concentrating on pressure driven instabilities.*

- **Mercier criterion** (local to magnetic surfaces):

    $\Rightarrow$ *local criterion on pressure driven modes, contained in ballooning procedure.*

- **Numerical work** (global waves and instabilities):

    $\Rightarrow$ *exploiting quadratic forms by means of Galerkin method.*

## Alfvén and slow continuum modes

- **Magnetic surface resonances** (limit $D \to \infty$):

$$D^\dagger X \approx -\frac{1}{\gamma p + B^2}\Big[\, G\frac{\gamma p + B^2}{B}Y + \gamma p F Z \,\Big]. \tag{6}$$

Substituting into second and third component of Eq. (5) leads to a system of two differential equations for $Y$ and $Z$ where the normal derivative no longer appears.

- $\Rightarrow$ **Modes localised about single magnetic surface:**

$$\boldsymbol{\xi}(\psi, \vartheta, \varphi) \approx -\mathrm{i}\delta(\psi - \psi_0)\,[\,\eta(\vartheta)\boldsymbol{\pi} + \zeta(\vartheta)\mathbf{b}\,]\,\mathrm{e}^{in\varphi}, \tag{7}$$

where the two tangential components

$$\eta \equiv \boldsymbol{\xi} \cdot \boldsymbol{\pi} \equiv -\mathrm{i}RB_p Y\,, \qquad \zeta \equiv \boldsymbol{\xi} \cdot \mathbf{b} \equiv -\mathrm{i}Z\,,$$

satisfy a system of two ODEs (repeated on next page):

$$\begin{pmatrix} \alpha_{11} & \alpha_{12} \\ \alpha_{21} & \alpha_{22} \end{pmatrix} \begin{pmatrix} \eta \\ \zeta \end{pmatrix} = \rho\omega^2 \begin{pmatrix} \eta \\ \zeta \end{pmatrix}.$$

## Alfvén and slow continuum modes (cont'd)

- Tangential components satisfy a system of two ODEs:

<div align="right">[Goedbloed, Phys. Fluids <b>18</b>, 1258 (1975)]</div>

$$\begin{pmatrix} \alpha_{11} & \alpha_{12} \\ \alpha_{21} & \alpha_{22} \end{pmatrix} \begin{pmatrix} \eta \\ \zeta \end{pmatrix} = \rho\omega^2 \begin{pmatrix} \eta \\ \zeta \end{pmatrix}, \tag{8}$$

where

$$\alpha_{11} \equiv \frac{B}{RB_p} F \frac{R^2 B_p^2}{B^2} F \frac{B}{RB_p} + \frac{4\gamma p B^2}{\gamma p + B^2} \kappa_g^2, \qquad \alpha_{12} \equiv -\mathrm{i} \frac{2\gamma p B^2}{\gamma p + B^2} \kappa_g F \frac{1}{B},$$

$$\alpha_{21} \equiv \mathrm{i} \frac{1}{B} F \frac{2\gamma p B^2}{\gamma p + B^2} \kappa_g, \qquad \alpha_{22} \equiv \frac{1}{B} F \frac{\gamma p B^2}{\gamma p + B^2} F \frac{1}{B}.$$

- Two coupled ODEs $\Rightarrow$ **Toroidal Alfvén and slow continuum modes**.

- Cylindrical limit $(\epsilon \to 0)$:

$$\omega_A = (m + nq)\, B_\theta/(r\sqrt{\rho}), \quad \eta_A \sim \delta(r - r_A),$$

$$\omega_S = \sqrt{\gamma p/(\gamma p + B^2)}\, \omega_A, \quad \zeta_S \sim \delta(r - r_S). \tag{9}$$

## Continuous spectrum

Numerical solution yields **continua with gaps:**                    [Poedts et al, PPCF **34**, 1397 (1992)]
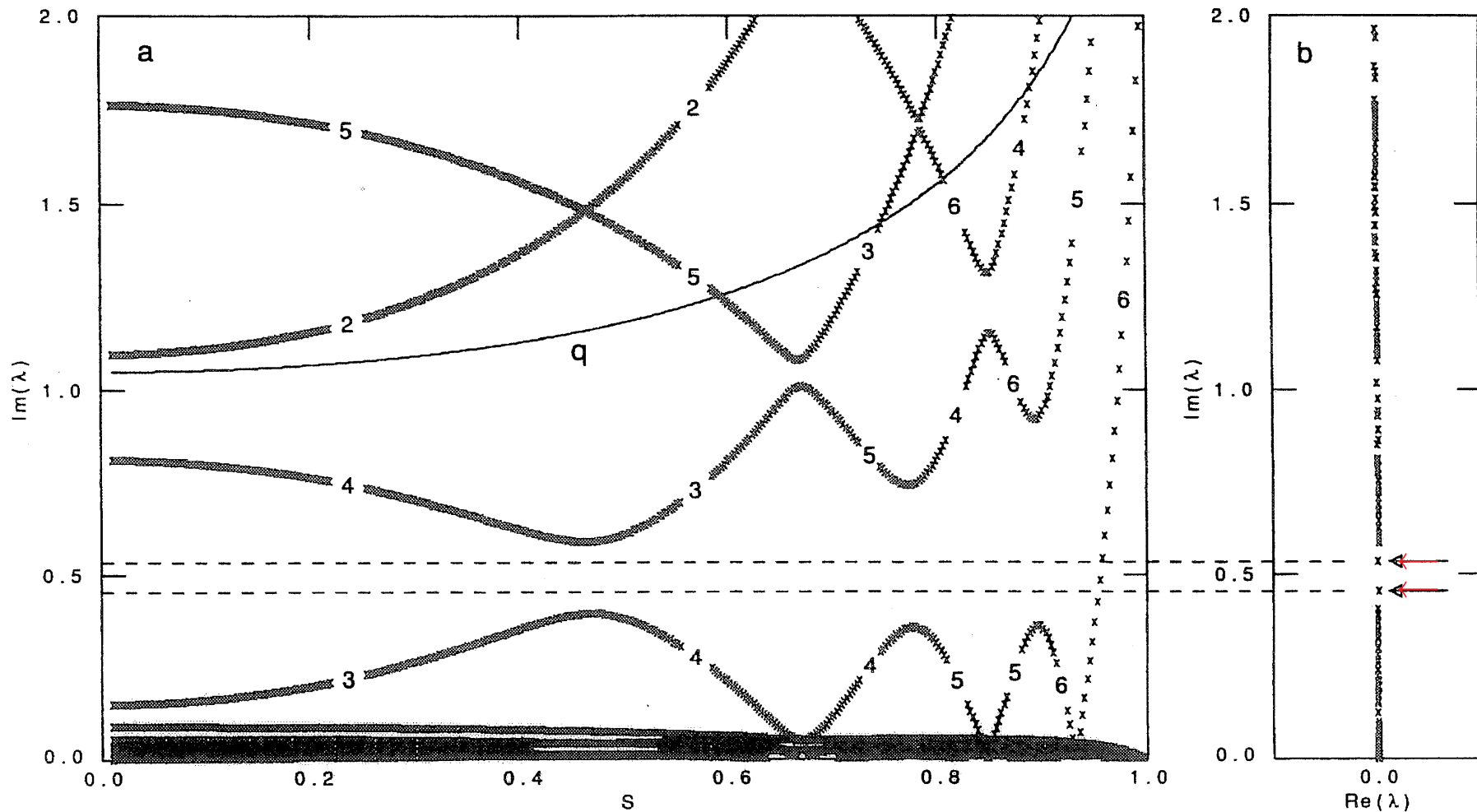


In those gaps, **Toroidal Alfvén Eigenmodes (TAEs).**

## Alfvén and slow ballooning modes

- **Magnetic field line resonances**: Reconcile field line localisation with poloidal and toroidal periodicity by means of **ballooning transformation** to extended poloidal angle $-\infty < \vartheta < \infty$. [Connor, Hastie, Taylor, Proc. Roy. Soc. **A365**, 1 (1999)]

  Ballooning modes are WKB solutions on that extended domain:

$$\boldsymbol{\xi}(\psi, \vartheta, \varphi) = \widetilde{\boldsymbol{\xi}}(\psi, \vartheta)\, \mathrm{e}^{inS(\psi, \vartheta, \varphi)}\,, \tag{10}$$

  where $n \gg 1$, and the eikonal

$$S \equiv \varphi - q(\vartheta - \vartheta_0)\,. \tag{11}$$

- Renormalise local wave number $\mathbf{k}_\perp = n\nabla S$ (i.e. $\perp \mathbf{B}$, but not $\perp$ magnetic surface):

$$\bar{\mathbf{k}} \equiv \mathbf{k}_\perp / n = \nabla S = \bar{k}_n \mathbf{n} + \bar{k}_\pi \boldsymbol{\pi}\,,$$

$$\bar{k}_n = -RB_p\left[q'(\vartheta - \vartheta_0) - (g_{12}/g_{22})q\right]\,, \qquad \bar{k}_\pi = -B/(RB_p)\,. \tag{12}$$

- Project on the related orthogonal triad, $\mathbf{e} \equiv \mathbf{k}_\perp / k_\perp\,, \mathbf{d}\,, \mathbf{b}$:

  $\Rightarrow$ new components $\tilde{u}, \tilde{v}, \tilde{\zeta}$ of the vector $\boldsymbol{\xi}$.

## Alfvén and slow ballooning modes (cont'd)

- Ballooning modes are perpendicular to $\mathbf{k}_\perp$, $\tilde{u} \equiv \mathrm{i}\mathbf{e} \cdot \boldsymbol{\xi} \approx 0$, i.e. they are described by two components,

$$\widetilde{\boldsymbol{\xi}}(\psi, \vartheta) \approx -\mathrm{i}\left[\tilde{v}(\psi, \vartheta)\mathbf{d} + \tilde{\zeta}(\psi, \vartheta)\mathbf{b}\right], \tag{13}$$

- which satisfy a *system of two ODEs:*     [Dewar & Glasser, Phys. Fluids **26**, 3038 (1983)]

$$\begin{pmatrix} \tilde{\alpha}_{11} & \tilde{\alpha}_{12} \\ \tilde{\alpha}_{21} & \tilde{\alpha}_{22} \end{pmatrix} \begin{pmatrix} \tilde{v} \\ \tilde{\zeta} \end{pmatrix} = \rho\omega^2 \begin{pmatrix} \tilde{v} \\ \tilde{\zeta} \end{pmatrix}, \tag{14}$$

$$\tilde{\alpha}_{11} \equiv \frac{B}{\bar{k}}\tilde{F}\frac{\bar{k}^2}{B^2}\tilde{F}\frac{B}{\bar{k}} + \frac{4\gamma pB^2}{\gamma p + B^2}\kappa_d^2 - 2\frac{B}{\bar{k}}\kappa_d\, p', \quad \tilde{\alpha}_{12} \equiv -\mathrm{i}\frac{2\gamma pB^2}{\gamma p + B^2}\kappa_d\tilde{F}\frac{1}{B},$$

$$\tilde{\alpha}_{21} \equiv \mathrm{i}\frac{1}{B}\tilde{F}\frac{2\gamma pB^2}{\gamma p + B^2}\kappa_d, \qquad\qquad \tilde{\alpha}_{22} \equiv \frac{1}{B}\tilde{F}\frac{\gamma pB^2}{\gamma p + B^2}\tilde{F}\frac{1}{B}. \tag{15}$$

- Two coupled ODEs $\Rightarrow$ **Toroidal Alfvén and slow ballooning modes**.

- Ballooning modes in tokamaks: **instabilities at high beta driven by the pressure gradient $p'$ and the curvature of the field lines**.

## Two directions in local analysis

- **Stability of tokamaks**: ballooning term $\kappa_d\, p' \approx \kappa_t\, p'$ dominates

  (instability searches out the worst conditions for confinement).

- **Alfvén wave heating**: ballooning term $\kappa_d\, p'$ unimportant

  (excitation forces stable waves of a fixed frequency onto the system).

## Mercier criterion

- Derived by Mercier, Nucl. Fusion **1**, 47 (1960), generalisation of Suydam criterion.

  (New interpretion: condition for *clustering of ballooning solutions* for $\vartheta \to \infty$.)

- The following expression is obtained:

$$\left[ \pi q' - I p' \oint \frac{1}{R^2 B_p^2} J d\vartheta \right]^2 + p' \oint \frac{B^2}{R^2 B_p^2} J d\vartheta$$

$$\times \left[ 2 \oint \frac{\kappa_p}{R B_p} J d\vartheta + I I' \oint \frac{1}{R^2 B_p^2} J d\vartheta \right] > 0 \,. \tag{16}$$

## Solving the full problem

- **Global analysis is necessarily numerical**

- **Ideal MHD codes:** ERATO, PEST, . . .

  [Appert, Berger, Gruber & Rappaz, JCP **18**, 284 (1975)]

  [Grimm, Greene & Johnson, Methods Comp. Phys. **16**, 253 (1976)]

- **Resistive MHD codes:** NOVA, CASTOR, MARS, . . .

  Will show results of CASTOR

  [Kerner, Goedbloed, Huysmans, Poedts & Schwarz, JCP **142**, 271 (1998)]

## Ideal MHD: Troyon limit

- **Numerically obtained theoretical limit for kink & ballooning stability:**

$$\beta\,(\%) < g_{\mathrm{T}}\frac{I\,(\mathrm{MA})}{a\,(\mathrm{m})\,B\,(\mathrm{T})}\,.$$

- But experimental points cross the curve!

- Present experimental limit (DIIID) :

$$\beta \sim 10\%\,.$$
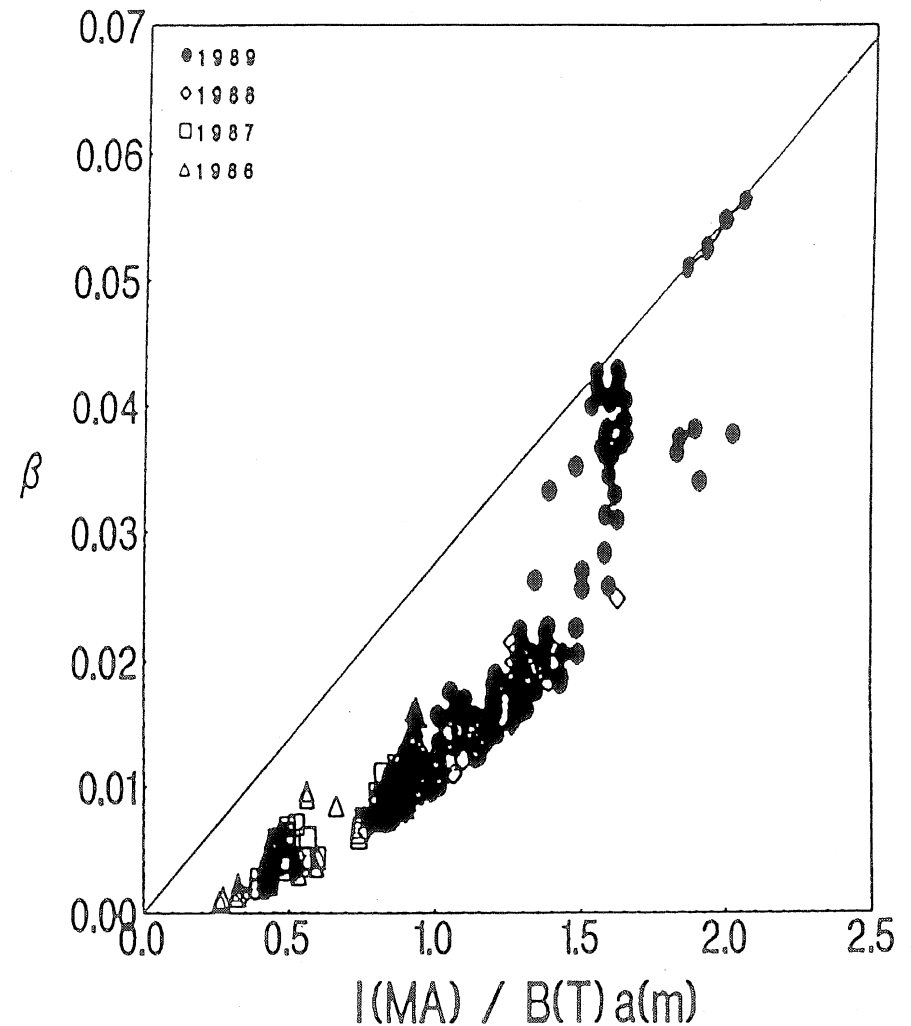
## Linearised Resistive MHD equations

- Dissipative MHD : *variable $\boldsymbol{\xi}$ no longer useful* since it is based on flux conservation.

  $\Rightarrow$ Return to *primitive variables* of resistive MHD, but get rid of $\nabla \cdot \mathbf{B}_1 = 0$ constraint by exploiting vector potential $\mathbf{A}_1$.

- **Resistive eigenvalue problem :**

$$\lambda \rho_1 = -\nabla \cdot (\rho \mathbf{v}_1),$$

$$\lambda \rho \mathbf{v}_1 = -\nabla \left( \rho\, T_1 + \frac{p}{\rho}\, \rho_1 \right) + (\nabla \times \mathbf{B}) \times (\nabla \times \mathbf{A}_1) - \mathbf{B} \times (\nabla \times \nabla \times \mathbf{A}_1),$$

$$\lambda \rho T_1 = -\rho \mathbf{v}_1 \cdot \nabla \left( \frac{p}{\rho} \right) - p \nabla \cdot \mathbf{v}_1 + 2\eta\,(\gamma - 1)\,(\nabla \times \mathbf{B}) \cdot (\nabla \times \nabla \times \mathbf{A}_1),$$

$$\lambda \mathbf{A}_1 = -\mathbf{B} \times \mathbf{v}_1 - \eta\, \nabla \times \nabla \times \mathbf{A}_1. \tag{17}$$

- Basic state represented by 8-vector :

$$\mathbf{U} \equiv [\, \rho_1, \mathbf{v}_1, T_1, \mathbf{A}_1 \,]^{\mathrm{T}}, \tag{18}$$

## Two Approaches

- **Conservative, ideal MHD** with $\mathbf{v}_1 \equiv \partial \boldsymbol{\xi} / \partial t$ :

$$\mathbf{F}(\boldsymbol{\xi}) = \rho \frac{\partial^2 \boldsymbol{\xi}}{\partial t^2} = -\rho \omega^2 \boldsymbol{\xi} \,, \tag{19}$$

where $\mathbf{F}$ is self-adjoint and the eigenvalues $\omega^2$ are real.

- **Dissipative, resistive MHD** with $\mathbf{U} \equiv [\rho_1, \mathbf{v}_1, T_1, \mathbf{B}_1]^T$:

$$\mathbf{L} \cdot \mathbf{U} = \mathbf{R} \cdot \frac{\partial \mathbf{U}}{\partial t} = \lambda \, \mathbf{R} \cdot \mathbf{U} \,, \tag{20}$$

where $\mathbf{L}$ is non-Hermitian and the eigenvalues $\lambda \equiv -\mathrm{i}\,\omega$ are complex.

## CASTOR & POLLUX: fusion & solar applications

[POLLUX (lied-tied coronal loop: Van der Linden, Goossens & Kerner, CPC **140**, 61 (1990)]

[CASTOR (tokamak): Kerner, Goedbloed, Huysmans, Poedts & Schwarz, JCP **142**, 271 (1998)]

- Resistive eigenvalue problem $\mathbf{L} \cdot \mathbf{U} = \lambda \, \mathbf{R} \cdot \mathbf{U}$ solved by **Galerkin method:**

$$\int \mathbf{V}^{\mathrm{T}} \cdot \mathbf{L} \cdot \mathbf{U} \, dV = \lambda \int \mathbf{V}^{\mathrm{T}} \cdot \mathbf{R} \cdot \mathbf{U} \, dV \,. \tag{21}$$

- FEM $(r)$ and FFT $(\vartheta)$ discretisation of $\mathbf{U}$ and $\mathbf{V}$:

$$\mathbf{A} \cdot \mathbf{x} = -\lambda \, \mathbf{B} \cdot \mathbf{x} \,, \tag{22}$$

  where $\mathbf{A}$ and $\mathbf{B}$ are large non-Hermitian matrices.

- **Eigenvalue problem** can be solved by several methods, the most effective one being Jacobi–Davidson.           [Sleijpen & van der Vorst, SIAM J. Matrix Anal. Appl. **17**, 401 (1996)]

- **External excitation** of modes leads to another discrete problem with large matrices:

$$(\mathbf{A} + \mathrm{i}\, \omega_d \mathbf{B}) \cdot \mathbf{x} = \mathbf{f} \,, \tag{23}$$

  with driving frequency $\omega_d$ and forcing term $\mathbf{f}$. (Used in MHD spectroscopy.)

# CASTOR dicretization
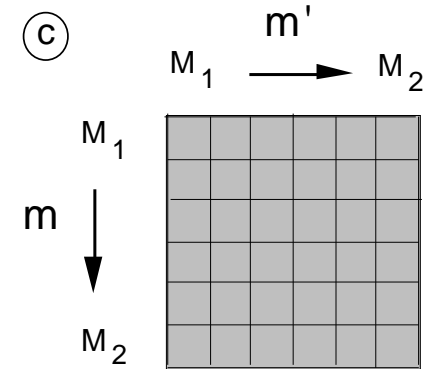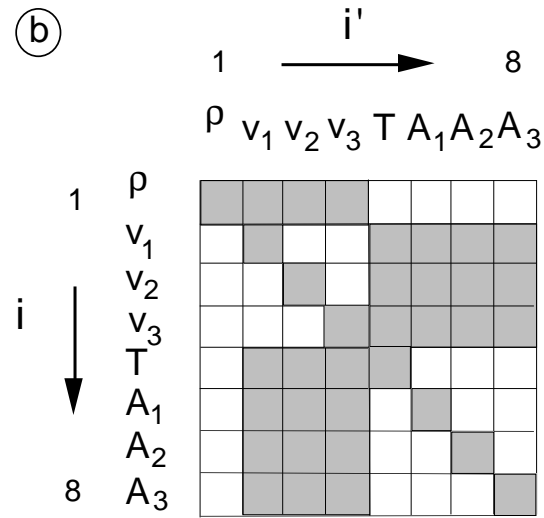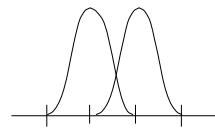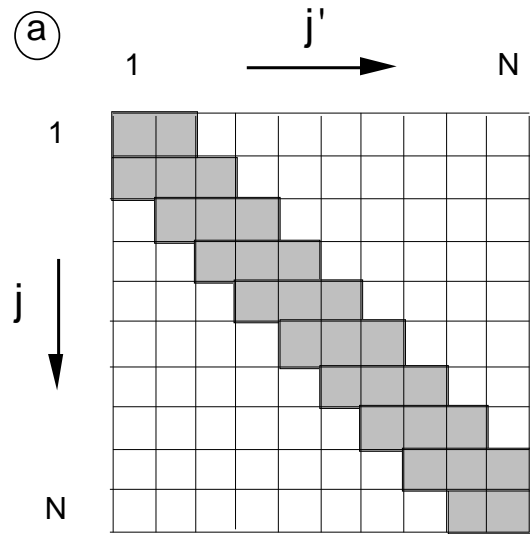
## Typical MHD stability study

- **ELMs in JET :**

  Playing with the equilibrium profiles, edge current density $j_\varphi$ (JET # 23336)

  $\Rightarrow n = 1$ free-boundary tearing modes,

  $\Rightarrow n = 4$ pressure-driven modes.

- General philosophy :

  Comparing experimental data on instabilities with theoretical results

  $\Rightarrow$ **MHD Spectroscopy.**

## Free-boundary tearing mode

- Flux averaged toroidal current profiles and corresponding growth rates as a function of the resistivity for the $n = 1$ free boundary tearing mode.
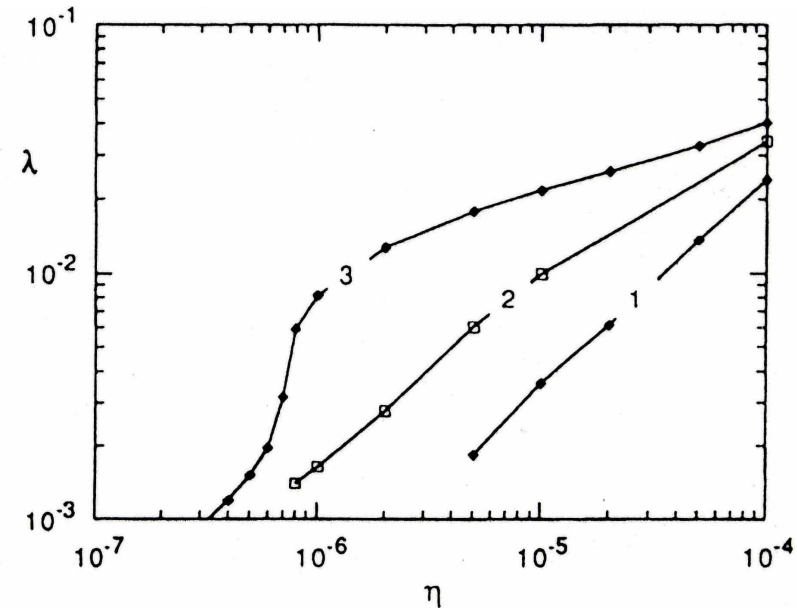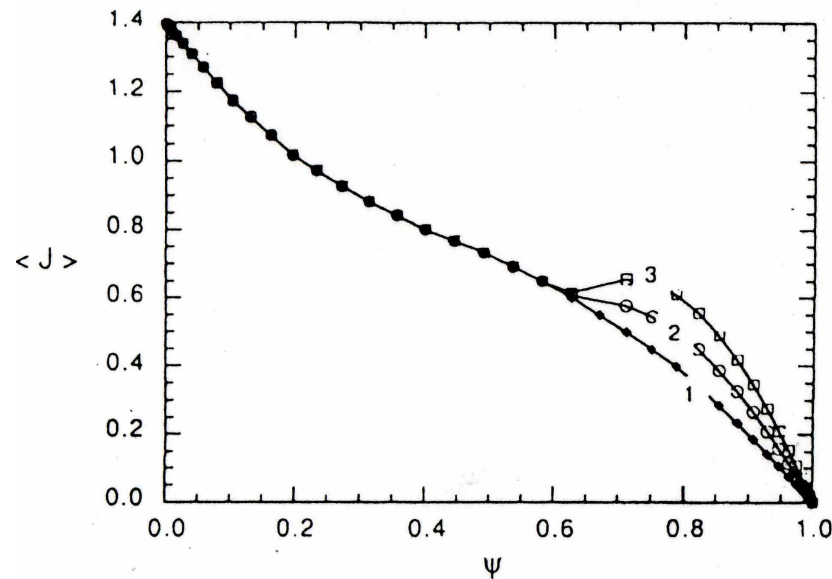


- Reconstructed profile (labelled by 1) produces growth rate that is insignificant for the relevant values of the edge resistivity. Artificial increase of the shoulder on the current density profile (curve labelled by 3) produces large growth rates with threshold that *could facilitate ELMs by sudden increase of resistivity due to edge cooling.*

[Huysmans, de Blank, Kerner, Goedbloed & Nave, EPS Conf. Innsbruck **I**, 247 (1992)]

# Internal/external resistive mode

Poloidal velocities of an $n = 4$ resistive mode (JET discharge # 27793):

*Internal resistive mode* at $q = 3$ (left), *becomes external for larger current* (right).
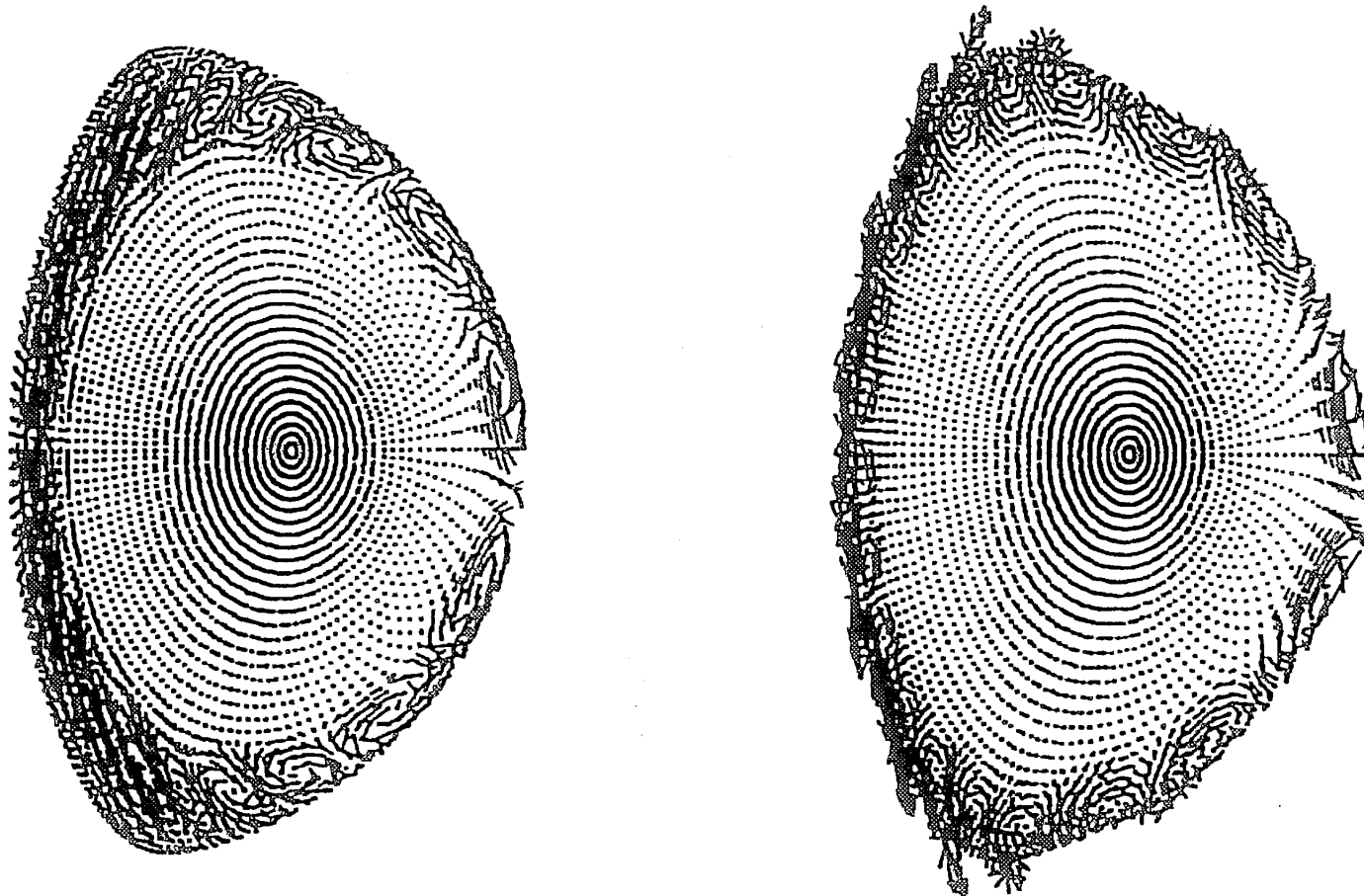


[Goedbloed, Huysmans, Holties, Kerner & Poedts, PPCF **35**, B277 (1993)]

## MHD spectroscopy

- *Computed response to $n = 1$ field perturbation induced by saddle coils at JET:*

  TAE (toroidicity $\Delta m = 1$), EAE (ellipticity $\Delta m = 2$) and BAE ($\beta$ induced):
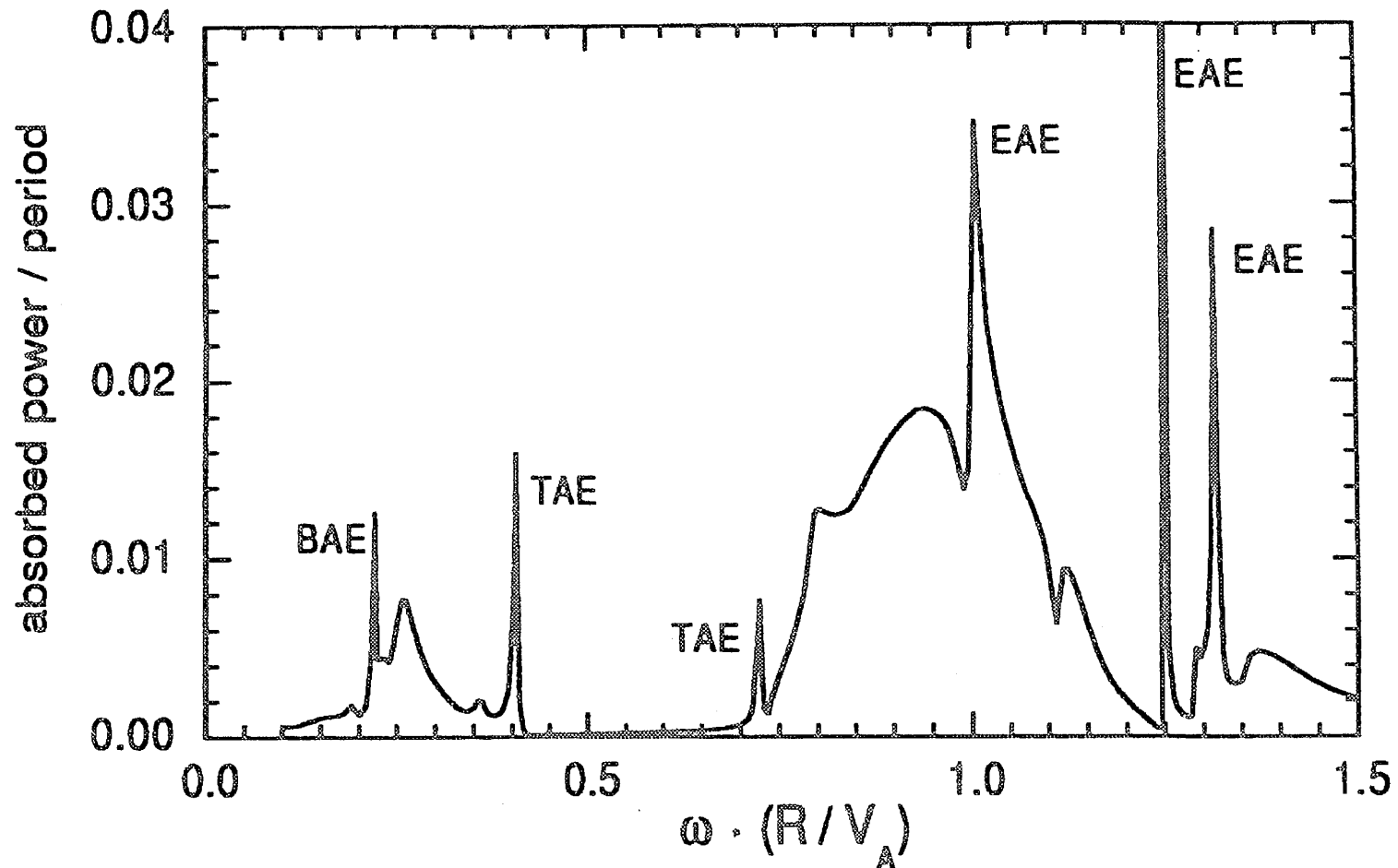


[Huysmans, Kerner, Borba, Holties & Goedbloed, PoP **2**, 1605 (1995)]

## MHD spectroscopy: Audible!

**Music of the tokamak**  (SOUND.WAV)

**MHD wave signals picked up by an external coil,**

**with artificial decrease ($10^{-3}$) of the frequency**

**(sound track Igor Semenov, Moscow)**